

# INVESTIGATION OF STRAIN-INDUCED BRAIN INJURY MECHANISM IN SIMULATED CAR ACCIDENTS

**Toshiyuki, Yanaoka Yukou, Takahashi Hisaki, Sugaya Takayuki, Kawabuchi**

Honda R&D Co., Ltd. Automobile R&D Center

Japan

Paper Number 19-0070

## ABSTRACT

Further reduction of brain injuries is crucial to diminish traffic fatalities. Past studies suggest that strain of incompressible brain tissue is generated mainly due to head rotation. Accident statistics show a higher rate of pedestrian fatalities resulting from strain-induced brain injuries in accidents with AIS 2+ brain injuries than that of car occupants. One factor for this difference would be larger translation and rotation of an unrestrained pedestrian body than those of a restrained car occupant. This study aimed to clarify the influence of whole body kinematics on the brain strain in pedestrians and occupants.

Time histories of the head translational and rotational accelerations were taken from the NHTSA crash test database for full frontal and MDB side impacts. Pedestrian crash simulations were conducted for frontal and side impacts using a human, small-sedan and SUV FE models to obtain head acceleration time histories. These time histories were applied to the skull of the GHBMC head/brain model. The time histories of the maximum principal strain from the GHBMC model were compared between occupants and pedestrians in the same impact direction. The body kinematics and the rotational velocity of the head were also compared to identify factors for the difference in the time history patterns of the maximum principal strain. In addition, these time histories were compared to that of the CIBIC (Convolution of Impulse response for Brain Injury Criterion) criterion developed in a previous study under each of the four conditions.

Peaks of brain strain were identified in both head pre-impact and impact phase for pedestrian while that was identified only in head impact phase for occupant, regardless of the impact direction. The flip of the rotational direction of the head in the head pre-impact phase was found only in pedestrian, likely resulting in the peak of brain strain prior to the head impact. This trend applied regardless of the direction of impact. The time history of the CIBIC criterion provided waveform patterns similar to the maximum principal strain time history in all impact conditions.

Peaks of brain strain in both head pre-impact and impact phase in pedestrian identified in this study would require reduction of peaks in both phases. A criterion predicting time history of brain strain, such as CIBIC, was found to be an effective tool to address reduction of peaks in multiple phases seen in pedestrian. These findings would lead to novel pedestrian safety technologies that control pedestrian kinematics to reduce the primary peak.

## INTRODUCTION

According to the data from National Automotive Sampling System (NASS) Crashworthiness Data System (CDS) from 2010 to 2015 and Pedestrian Crash Data Study (PCDS) from 1994 to 1998, among fatal accidents, the most frequent injuries that sustain the Maximum Abbreviated Injury Scale (MAIS) are head injuries (33% for car occupants, 46% for pedestrians). Of those head injuries, the percentage of fatalities due to brain injuries is 78% for car occupants and 81% for pedestrians. These data indicate that reduction of brain injuries is crucial to reducing traffic fatalities.

Although brain injuries involve numerous injury patterns, they can be broadly classified into the three types; 1) focal injuries due to pressure and/or skull fracture (contusion and epidural hematoma), 2) injuries due to relative displacement of the brain and the skull (subdural hematoma), and 3) strain-induced brain injuries (subarachnoid hemorrhage, intracranial hemorrhage and diffuse axonal injury). The data from NASS CDS from 2010 to 2015 and PCDS from 1994 to 1998 show strain-induced brain injuries account for the largest percentage of fatalities due to

brain injuries, at 81% of car occupants and 73% of pedestrians. In addition, the percentage of fatalities due to strain-induced brain injuries in cases of AIS 2+ brain injuries is 17% for pedestrians and 8% for car occupants. Previous research (Holbourn et al.[1]) suggested that since the brain is incompressible, brain strain occurs mainly due to rotational inputs. One reason for this high rate of fatality caused by strain-induced brain injuries in pedestrian accidents may be the much larger movement and rotation of a pedestrian's head in a crash compared to that of a car occupant. Therefore, it is important to clarify the influence of difference in whole-body kinematics between pedestrians and car occupants on the brain strain.

Most previous research focusing on strain-induced brain injuries investigated criteria for predicting the maximum value of brain strain by applying the rigid body kinematics of the head to human head/brain FE models [2-6]. There are few known studies that focused on the time histories of brain strain needed to clarify the relationship between whole-body kinematics and brain strain. Takahashi et al. [7] and Gabler et al. [8] developed a criterion capable of simulating not only the maximum value but also the time history of brain strain, by representing the complex brain response characteristics with a simple physical model. However, these studies did not investigate characteristics of the time histories of their criteria for pedestrians and car occupants with respect to whole-body kinematics.

This study aimed to clarify the influence of whole-body kinematics on the brain strain in pedestrians and car occupants. The time history of brain strain was obtained by applying the rigid-body head kinematics obtained from representative load cases for car occupants and pedestrians to a human head/brain FE model. The relationship between whole-body kinematics and time history of brain strain was investigated. In addition, the effectiveness of an existing prediction method for time histories of brain strain to capture their characteristics was validated by comparing against brain strain time histories obtained from a human head/brain FE model.

## METHOD

### Relationship between Brain Strain and Kinematics

The relationship between whole-body kinematics and time history of brain strain was investigated in representative load cases of car occupants and pedestrians. Frontal and side impacts to the body were investigated for both car occupants and pedestrians to clarify the influence of the impact direction.

**Time history of head acceleration:** For occupant, head translational and rotational acceleration data of the drivers and video of car occupant kinematics were obtained from the National Highway Traffic Safety Administration (NHTSA) Vehicle Crash Test Database. Full frontal impact tests at 56 km/h and moving deformable barrier (MDB) side impact tests at 62 km/h performed by NHTSA for the United States New Car Assessment Program (US NCAP) were selected for the load cases for frontal and side impact to the body, respectively. In order to confirm the influence at various levels of brain strain, two cases approximating the maximum and minimum rotational acceleration were selected for each impact configuration (full frontal impact and MDB side impact) from among the data in the NHTSA Vehicle Crash Test Database. Cases where video of car occupant kinematics is not available and cases involving head impact with components other than airbags were excluded. The selected cases are shown in Table 1.

**Table 1**  
**Selected cases for occupant**

Case ID	Crash Mode	NHTSA Test ID
OF1	Full frontal 56km/h	8156
OF2	Full frontal 56km/h	8314
OS1	MDB side impact 62km/h	7981
OS2	MDB side impact 62km/h	7984

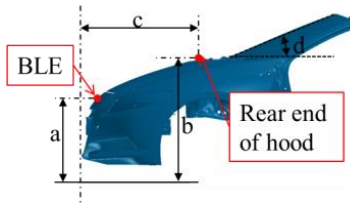
For pedestrian, time histories of the head translational and rotational accelerations and video of pedestrian kinematics were obtained from the impact simulation to the front and side of a pedestrian at 40 km/h using a human

and a car FE model. In order to compare the kinematics between car occupants and pedestrians, the human FE model representing the size of average American male (AM50) developed by Takahashi et al. [9] was used to match the size of the occupant dummies used in US NCAP. This model has been validated at the component level for each of the neck, chest, pelvis, thigh, knee, and leg, and also for whole-body kinematics. A mid-gait stance was used to represent a lower limb posture with the limbs apart, as the limbs are not aligned in most of the time in a gait cycle. Since car shape strongly influences whole-body kinematics of a pedestrian, two production car FE models representing a small sedan (Car1) and an SUV (Car2) were used. The vehicle models were composed of the components needed to investigate the whole-body kinematics and head acceleration time histories, including body frame, bumper, hood, fenders, cowl top panel and windshield. The components not needed in this study were modeled as a rigid-body which consisted of a node located at the center of gravity of the car and the nodes located at the rear end of body frame. The total mass of the car model was adjusted to match the mass of the car with two occupants on board by adding the mass to the node located at the center of gravity of car. The initial velocity of the car model was set to 40km/h to simulate car-to-pedestrian impact. The car-to-pedestrian impact simulations were conducted until the end of head contact to the car. The time histories of translational and rotational acceleration of the head, and video data which shows the whole-body kinematics were obtained from the pedestrian impact simulations. Figure 1 shows the side view of car FE models used in this study and Table 2 shows dimensions of bonnet leading edge (BLE), rear end of hood at lateral center of the car and windshield angle. The combination of car FE models and impact directions for impact simulations are shown in Table 3.



Figure 1. Side view of car FE models

Table 2  
Dimensions of BLE, rear end of hood at lateral center of the car and windshield angle



ID	Description	Car1	Car2
a	Height of BLE from ground [mm]	602	907
b	Height of rear end of hood from ground [mm]	904	1053
c	Longitudinal distance from car front end to rear end of hood [mm]	874	930
d	Windshield angle relative to ground[deg]	22	31

Table 3  
Pedestrian impact configurations

CaseID	Impact Direction	Car Model
PF1	Frontal	Car1
PF2	Frontal	Car2
PS1	Side	Car1
PS2	Side	Car2

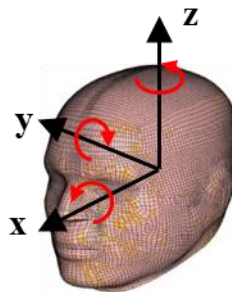
**Time history of brain strain:** The Global Human Body Models Consortium (GHBM) head/brain FE model developed by Mao et al. [10] was used in this study. This model reproduces the brain structure in detail, and displacement and pressure response has been validated against the results of dynamic loading test using PMHSs.

Figure 4 shows the mid-sagittal section of the model. Although deformable material was used for flesh, facial bones and skull in the original model, these components were changed from deformable to rigid-body to investigate time histories of brain strain with respect to whole-body kinematics. Time histories of maximum principal strain (MPS) of all of the brain elements were obtained by applying time history data of head translational and rotational accelerations for car occupants and pedestrians to the rigid-body skull of the GHBMC head/brain FE model. The time history of MPS in the brain (hereafter called  $MPS_{\text{brain}}$ ) was calculated from the maximum of MPS value among the all of the brain elements in each time step. In addition, in order to represent the direction of head rotational motion, time histories of head rotational velocity were obtained from the simulation results for both car occupants and pedestrians.



**Figure 2. Mid-sagittal section of GHBMC head/brain FE model**

**Comparison of Kinematics with  $MPS_{\text{brain}}$ :** In order to investigate factors producing differences in the time history patterns of  $MPS_{\text{brain}}$ , time history of the rotational velocity of the head and kinematics of head and upper body were compared between car occupant and pedestrian. Since head contact timing from barrier or pedestrian contact timing was significantly different between car occupants and pedestrians, factors were investigated by dividing the time from the start of barrier or pedestrian contact to the end of head contact into following two time domains; 1) from the start of barrier or pedestrian contact to the start of head contact (hereafter called pre-impact phase) and 2) from the start of head contact to the end of head contact (hereafter called impact phase). The start and end of head contact was identified from the time history of the head acceleration. In order to compare the difference of kinematics between car occupants and pedestrians, same local coordinate system shown in Figure 3 was used for both car occupants and pedestrians.



**Figure 3. Local coordinate system used in this study**

**Comparison of Time Histories between CIBIC and  $MPS_{\text{brain}}$**

The time history of  $MPS_{\text{brain}}$  obtained from the GHBMC head/brain FE model was compared with that of an existing prediction method to validate the effectiveness for time histories of  $MPS_{\text{brain}}$  to capture their characteristics.

**Existing motion-based brain injury criterion (CIBIC):** By assuming that the strain response obtained from the GHBMC head/brain FE model can be reproduced by a simple one-dimensional linear viscoelastic model (Kelvin model) shown in Figure 4, Takahashi et al. [7] developed an injury criterion named CIBIC (Convolution of Impulse response for Brain Injury Criterion) that predicts the time histories of  $MPS_{\text{brain}}$ . CIBIC is expressed by the analytical solution of impulse response of the simple one-dimensional Kelvin model (Equations 1 and 2).

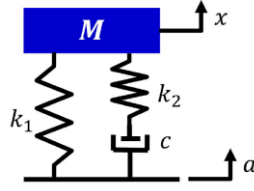


**Figure 4. Linear viscoelastic model (Kelvin model) used for development of CIBIC (Takahashi et al. [7])**

$$\mathbf{x}(t) = \mathbf{d}_1 e^{-a_1 t} - e^{-a_2 t} \{ \mathbf{d}_1 \cos(bt) + \mathbf{d}_2 \sin(bt) \} \quad (\text{Equation 1, Takahashi et al. [7]})$$

where  $a_1$ ,  $a_2$ ,  $d_1$ ,  $d_2$  and  $b$  is the coefficients identified from  $M$ ,  $k_1$ ,  $k_2$  and  $c$  in Figure 4 to represent rotational response of the GHBMC head/brain FE model when step function with a 1ms duration was applied to the model.

$$\text{CIBIC} = \sqrt{\sum_{i=1}^3 \left\{ \int_0^t x_i(t - \tau) \alpha_i(t) d\tau \right\}^2} \quad (\text{Equation 2, Takahashi et al. [7]})$$

where  $i=1,2,3$  represent the  $x$ ,  $y$  and  $z$  axis and  $\alpha_i$  is rotational acceleration.

CIBIC is a criterion that enables prediction of brain strain time histories, as expressed by Equation 2. Time histories of CIBIC were calculated by using the time histories of the head rotational acceleration in car occupant and pedestrian, and compared with the time histories of  $\text{MPS}_{\text{brain}}$  obtained from the GHBMC head/brain model.

## RESULTS

### Relationship between Brain Strain and Kinematics

Figures 5 and 6 show the comparison of the time history of  $\text{MPS}_{\text{brain}}$  between occupant and pedestrian for frontal and side impact cases, respectively. Comparison of time histories of rotational velocity between occupant and pedestrian for frontal and side impact are shown in Figures 7 and 8, respectively. Kinematics from video in occupant and pedestrian are compared in Figures 9 and 10 for frontal and side impact cases, respectively. All graphs are plotted from the start of barrier or pedestrian contact to the end of head contact, and values are normalized by the peak. The start time of head contact which divide time domain into pre-impact phase and impact phase is also plotted.

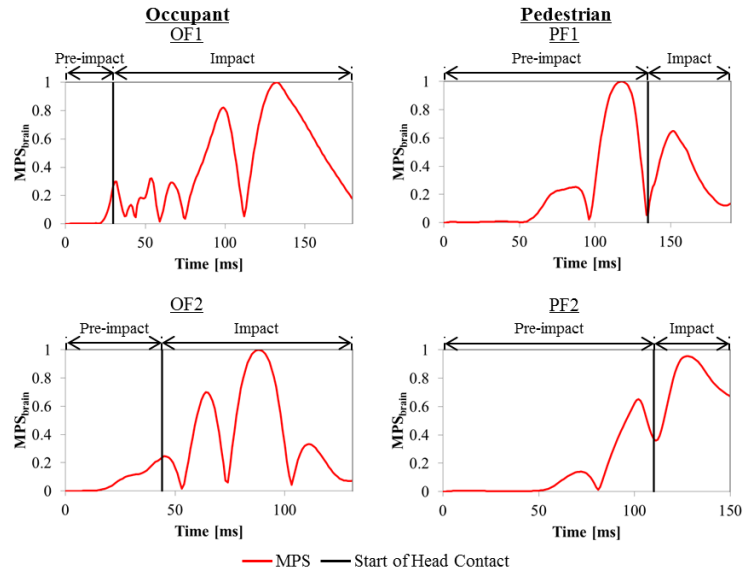


Figure 5. Comparison of time history of  $MPS_{brain}$  between car occupant and pedestrian in frontal impact

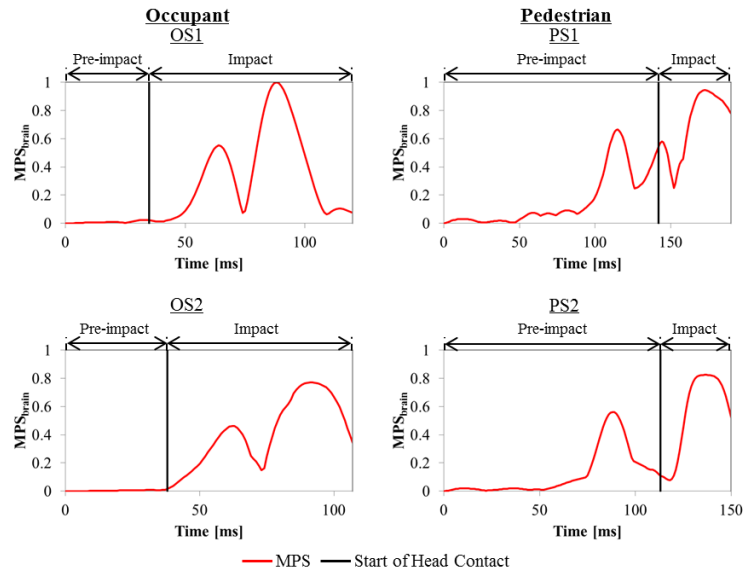
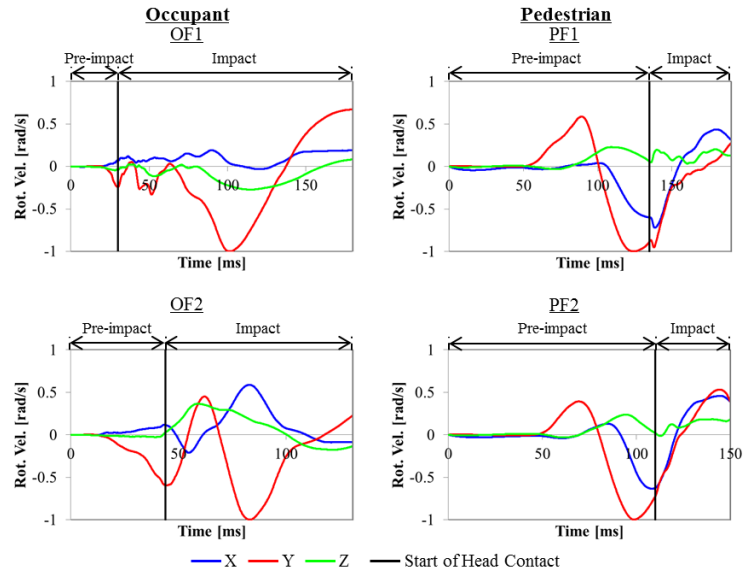
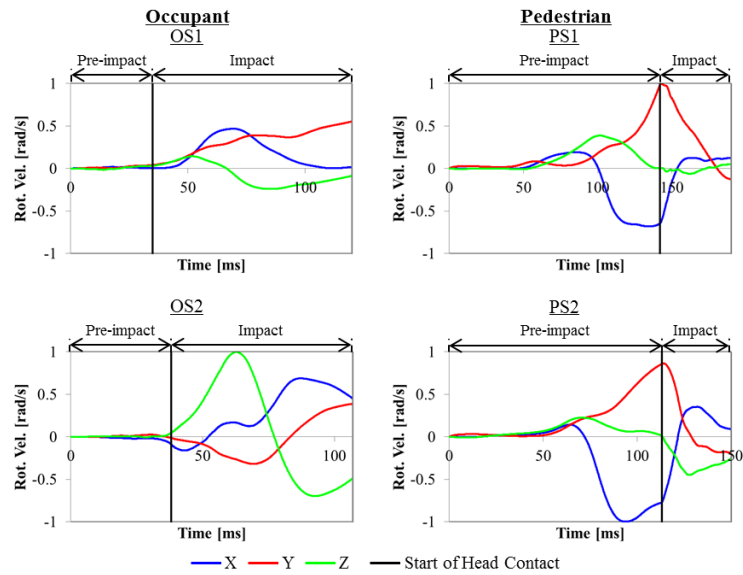


Figure 6. Comparison of time history of  $MPS_{brain}$  between car occupant and pedestrian in side impact



**Figure 7. Comparison of time history of rotational velocity between car occupant and pedestrian in frontal impact cases**



**Figure 8. Comparison of time history of rotational velocity between car occupant and pedestrian in side impact**

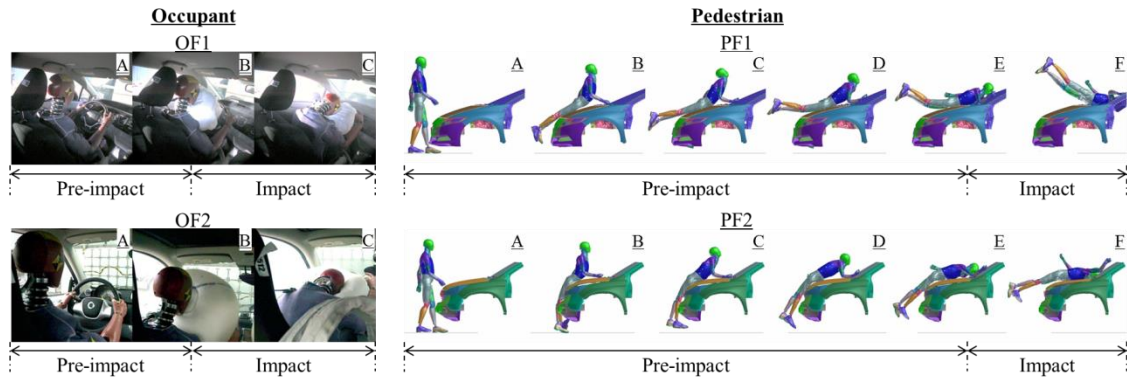


**Figure 9. Comparison of kinematics between occupant and pedestrian in frontal impact (For car occupant, A: initial state, B: start of head contact and C: end of head contact. For pedestrian, A: initial state, B: head rotation in opposite direction of the car surface, C: flip timing of head rotation, D: head rotation toward the car surface, E: start of head contact and F: end of head contact)**

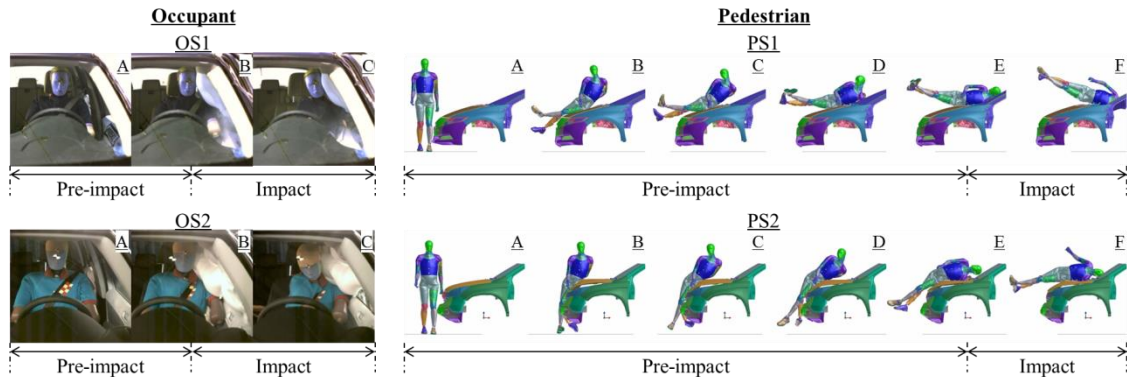


**Figure 10. Comparison of kinematics between occupant and pedestrian in side impact cases (For car occupant, A: initial state, B: start of head contact and C: end of head contact. For pedestrian, A: initial state, B: head rotation in opposite direction of the car surface, C: flip timing of head rotation, D: head rotation toward the car surface, E: start of head contact and F: end of head contact)**

### **Comparison of Time Histories between CIBIC and $MPS_{\text{brain}}$**

Figures 11 through 14 compare the time histories of  $MPS_{\text{brain}}$  obtained from the GHBM model and the time histories of CIBIC in full frontal impact, MDB side impact, pedestrian frontal impact and pedestrian side impact. All graphs are plotted from the start of barrier or pedestrian contact to the end of head contact, and values are normalized by the maximum value. The start time of head contact which divide time domain into pre-impact phase and impact phase is also plotted.

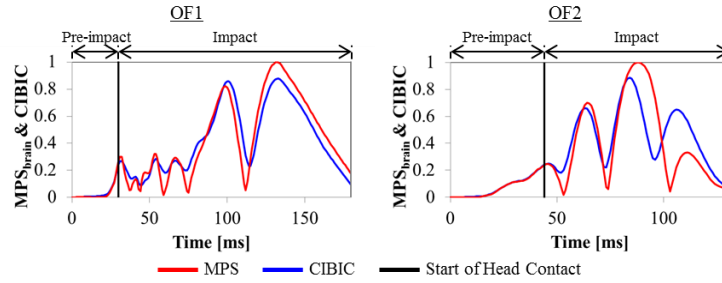


Figure 11. Comparison of time history of CIBIC with that of  $MPS_{brain}$  in full frontal impact

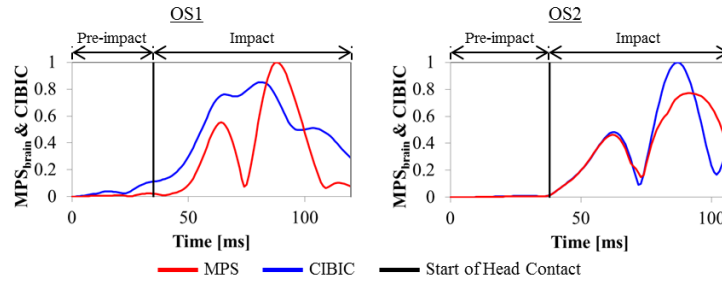


Figure 12. Comparison of time history of CIBIC with that of  $MPS_{brain}$  in MDB side impact

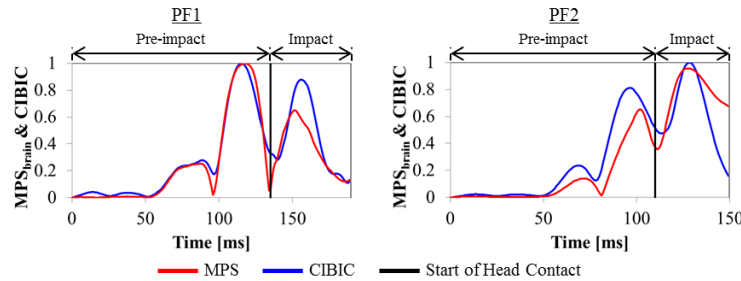


Figure 13. Comparison of time history of CIBIC with that of  $MPS_{brain}$  in pedestrian frontal impact

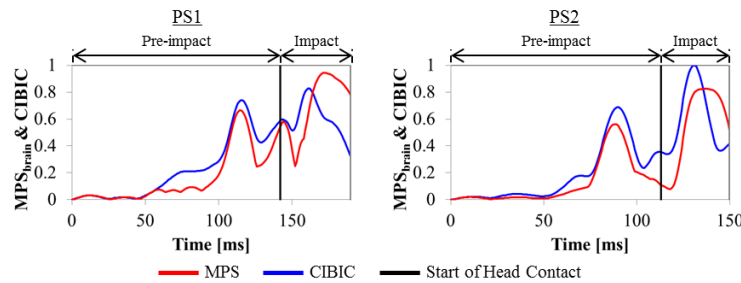


Figure 14. Comparison of time history of CIBIC with that of  $MPS_{brain}$  in pedestrian side impact

## DISCUSSION

Figures 5 and 6 show that, regardless of the impact direction, peaks of  $MPS_{brain}$  occur in both the pre-impact phase and the impact phase in the pedestrian impact cases while peaks of  $MPS_{brain}$  occur only in the impact phase for the car occupant impact cases. In addition, Figures 7 and 8 show that the sign of rotational velocity of dominant axis (Y

axis for frontal impact and X axis for side impact) flips in the pre-impact phase in the pedestrian impact cases, while this sign flip is not found in the car occupant impact cases. As shown in Figures 9 and 10, this tendency is also confirmed in the comparison of kinematics between car occupants and pedestrians. In addition, Figure 9 and 10 also show that, regardless of the impact direction, the rotation of upper body in the pre-impact phase in the pedestrian impact cases is significantly larger than that in the car occupant impact cases.

Since the head and upper body are connected by the flexible neck with a bending stiffness, the head rotates in the opposite direction relative to the upper body rotation due to the inertia of the head when the upper body inclines toward the car surface. Then, the rotational direction of the head flips by the reaction moment in the neck. Since brain has the inertia and softer material properties compared to the skull, peak of brain strain occurs with some delay relative to the flip timing of the rotational direction of the head (the zero-crossing time of the rotational velocity of the skull). As shown in Figures 9 and 10, since the rotation of upper body in the pre-impact phase in the pedestrian impact cases is significantly larger than that in the car occupant impact cases, these steps can occur during the pre-impact phase in the pedestrian impact cases. In addition, it is presumed that the change in the rotational velocity by the flip of the rotational direction of the head increases with the inclination of upper body. These are thought to be the reason why the pedestrian impact cases, which have flip of the rotational direction of the head due to large upper body inclination in the pre-impact phase, exhibit a large  $MPS_{\text{brain}}$  peak in this phase that does not occur for the car occupant impact cases. These results suggest that reduction of the probability of strain-induced brain injuries in pedestrians requires reduction of the peak  $MPS_{\text{brain}}$  in the pre-impact phase in addition to mitigating the impact force from the car body to the head in the impact phase. It is also suggested that pedestrian whole-body kinematics would need to be controlled to reduce the peak in pre-impact phase.

As shown in Figures 11 to 14, CIBIC accurately reproduces the  $MPS_{\text{brain}}$  response. Furthermore, as shown in Figures 12 and 13, CIBIC can reproduce the peak timing and value in the pre-impact phase of  $MPS_{\text{brain}}$  response which is typical response in the pedestrian impact. Since CIBIC is a criterion for predicting brain strain response using a simple physical model, it would be a criterion suitable for evaluating probability of injury with multiple peaks of brain strain.

It should be noted that the results of the current study depends on the validity of the FE models and crash test dummies. Further validation needs to be done once such simulation tools are improved in future studies.

## CONCLUSION

It was demonstrated that, unlike car occupants, the peak value of MPS in the brain occurs during both the pre-impact and impact phases regardless of the impact direction. The strain-induced brain injury criterion, CIBIC, was found to accurately reproduce the time history of MPS in the brain predicted by an FE head/brain model under full frontal impact, MDB side impact and pedestrian frontal and side impact conditions, showing applicability of CIBIC in evaluating strain in the brain with multiple peaks.

## REFERENCES

- [1] Holbourn, A.H.S. 1943. "Mechanics of head injuries." *Lancet* 2. October 9: 438-41
- [2] Kimpara, H., Nakahira, Y., Iwamoto, M., Rowson, S., Duma, S. 2011. "Head injury prediction method based on 6 degree of freedom head acceleration measurements during impact." *International Journal of Automotive Engineering*, 20114490
- [3] Kimpara, H. and Iwamoto, M. 2012. "Mild traumatic brain injury predictors based on angular accelerations during impacts." *Ann Biomed Eng.*, 40(1):114-26

- [4] Newman, J.A., Shewchenko, N., Welbourne, E. 2000. "A proposed new biomechanical head injury assessment function - the maximum power index." *Stapp Car Crash J.*, 44: 215-47
- [5] Takhounts, E.G., Craig, M.J., Moorhouse, K., McFadden, J., Hasija, V.2013. "Development of brain injury criteria (BrIC)." *Stapp Car Crash J.*, 57: 243-66
- [6] Yanaoka, T., Dokko, Y., Takahashi, Y. 2015. "Investigation on an injury criterion related to traumatic brain injury primarily induced by head rotation." *SAE International Technical Paper*, 2015-.01-1439
- [7] Gabler, L.F., Joodaki, H., Crandall, J.R., Panzer, M.B. 2018. "Development of a single-degree-of-freedom mechanical model for predicting strain-based brain injury response." *Journal of Biomechanical Engineering*, Vol.140, 031002
- [8] Takahashi, Y., Yanaoka, T. 2017. "A study of injury criteria for brain injuries in traffic accidents." Paper presented at: 25th ESV conference, Paper Number: 17-0040.
- [9] Takahashi Y., Asanuma H., Yanaoka T. 2015 "Development of a Full - Body Human FE Model for Pedestrian Crash Reconstructions." Paper presented at: IRCOBI Conference; 2015.
- [10] Mao H., Zhang L., Jiang B., Genthikatti V.V., Jin X., Zhu F., Makwana R., Gill A., Jandir G., Singh A., Yang K.H. 2013. "Development of a finite element human head model partially validated with thirty five experimental cases." *J Biomech Eng.*, 2013 Nov;135(11):111002.